Excited electronic states from a generalization of the extended Koopmans theorem

Y. Pavlyukh

Department of Physics and Research Center OPTIMAS, University of Kaiserslautern, P.O. Box 3049, 67653 Kaiserslautern, Germany and Institut für Physik, Martin-Luther-Universität Halle-Wittenberg, 06099 Halle, Germany

(Received 15 August 2018; published 16 November 2018)

Inspired by the extended Koopmans theorem, we demonstrate that excited electronic states can efficiently and very accurately be computed from the ground-state density correlators. That this is possible in principle does not come as a surprise. However, what correlator order is needed is an important question. There are a number of methods that differ in the way in which higher-order correlators, which are very expensive to evaluate, are treated: the equation-of-motion approach, also known as the random phase approximation, the cumulant, and the Hermitian operator methods. Here it is shown that there exists, in fact, a close connection between the extended Koopmans theorem and the equation-of-motion approach. A dramatic improvement over the conventional linear-response calculations is numerically demonstrated for a paradigmatic molecular system and explained by comparing with the equation-of-motion approach for a single-determinant reference state and for the case of composite excitations. Our approach opens prospects for systematic improvements of the adiabatic approximation of the time-dependent density functional theory by exploiting properties of the correlated ground state.

DOI: 10.1103/PhysRevA.98.052508

I. INTRODUCTION

Knowledge of excited electronic states in atoms, molecules, and extended systems is a cornerstone of fundamental materials science [1] having profound technological applications [2]. Time-dependent density functional theory (TDDFT) [3–6] has been universally used for the computation of neutral excited states demonstrating excellent compromise between the numerical effort and the accuracy, which is even comparable to the accuracy of dedicated but computationally more demanding methods [7–10].

Despite this impressive progress, there are classes of materials—remarkably light-harvesting complexes with paramount importance in biochemistry and technology [11,12]—that in principle cannot be described in the framework of the commonly used adiabatic approximation of TDDFT [13]. The difficulty is in the description of the doubly excited states and states in the vicinity of conical intersections where corresponding many-body wave functions are manifestly multideterminantal. Improvement of the Casida's linear response equations of TDDFT can be achieved by the explicit inclusion of double [14,15] and particle-particle [16] excitation channels, by working in the natural orbitals basis [17], or by using the ensemble DFT [18]. The time-dependent Sham-Schlüter equation allows us to construct the optimized effective potential systematically in the exact-exchange case [19] and for any given diagrammatic self-energy approximation [20]. Many-body perturbation theory and diagrammatic approach leads to methods based on the solution of the Bethe-Salpeter equation (BSE) [21–24]. However, all these methods share substantially higher computational complexity, and are often plagued with numerical instabilities [25–28]. In view of these methodological difficulties, insight on the computation of excited states from different theories is therefore called for.

In this work we take advantage of the density matrix formalism. This enables one to develop a systematic theoretical approach to include correlation effects in excited-state calculations on the basis of the ground-state reduced density matrices (RDMs). We bring together two approaches: the equation-of-motion (EOM) formalism [29] and the extended Koopmans theorem (EKT) [30], which is closely connected to the Hermitian operator method and its generalizations [31–33]. The first one states that excited states (with energy E_α and wave function $|\Psi_\alpha\rangle = \widehat{Q}_\alpha|\Psi_0\rangle$) can be determined from the eigenvalue equation

$$\langle[\widehat{A},[\widehat{H},\widehat{Q}_\alpha]]\rangle = (E_\alpha - E_0)\langle[\widehat{A},\widehat{Q}_\alpha]\rangle. \tag{1}$$

Here, the average with respect to the ground-state wave function $|\Psi_0\rangle$ involves commutators of the excitation operator $\widehat{Q}_\alpha$, the Hamiltonian of the system $\widehat{H}$, and arbitrary deexcitation operators $\widehat{A}$. This equation is valid provided that the consistency condition

$$\widehat{Q}_\alpha^\dagger|\Psi_0\rangle = 0 \tag{2}$$

holds. This is not true if $\widehat{Q}_\alpha^\dagger$ changes the number of particles in the system. However, for exact excitation operators $|\Psi_\alpha\rangle\langle\Psi_0|$ preserving the number of particles it is generally valid. Equation (2) is central for our discussion.

If in Eq. (1) we set $\widehat{Q}_\alpha^\dagger$ to be linear combinations of single excitation operators $\widehat{E}_{ij}^\sigma = \hat{c}_{i\sigma}^\dagger\hat{c}_{j\sigma}$, and assume that $|\Psi_0\rangle$ is given by a single Slater determinant, the random phase approximation (RPA) follows. However, Eq. (1) can be extended in several ways.

One possibility is to use the true correlated ground state. This leads to the so-called extended random phase approximation (ERPA). Besides single-particle properties as in RPA, the two-particle RDM (2-RDM) is now needed. It is a

complicated quantity. Different approaches for its computation give rise to different implementations of ERPA: for instance variational optimization by van Aggelen *et al.* [34] or the N-representable 2-RDM from the geminal theory by Chatterjee and Pernal [35].

The second possibility is to keep the ground state on a weakly correlated level, but to include double excitations in $\widehat{Q}_\alpha$. This idea has a very long history starting probably from the work of Wambach [36], who presented a very nice diagrammatic analysis of the involved physical processes: additional scattering channels arise by down-folding the total Hamiltonian onto the space of single excitations. The same idea was used by Maitra *et al.* [37] to include double excitations in the formalism of TDDFT. Subsequently Casida presented a mathematical substantiation of this approach [38], and Sangalli *et al.* [23] performed a diagrammatic analysis connecting it to BSE. They found that while kernel diagrams are included in ERPA, the self-energy diagrams are not. We will show below that it is directly related to the violation of the consistency condition (2). However, these two ways are not completely disconnected because higher-order excitations need to be added to ERPA in order to guarantee proper spin symmetries of excited states [39].

The extended Koopmans theorem does not rely on the assumption (2). The very first application goes back to Smith and Day, and was initially devised as a tool to obtain ionization potentials and electron affinities from the known ground state [30]. The central equation is very similar to EOM (1):

$$\langle \widehat{A}\,[\widehat{H}, \widehat{Q}_\alpha]\rangle = (E_\alpha - E_0)\langle \widehat{A}\,\widehat{Q}_\alpha\rangle. \tag{3}$$

As can be seen, the outer commutator is absent, therefore the consistency condition (2) is no longer required. In the theory of Smith and Day, dropping this condition was necessary for the description of processes changing number of particles since $\langle \Psi_\alpha^{(\pm)}|\Psi_0\rangle = 0$ could not be guaranteed. The method has been successfully used to determine spectroscopic properties of molecular systems [40–42], in particular, in conjunction with correlated Matsubara Green's function approach [43–46].

In the context of neutral excitations, Eq. (3) was used in several works: Rosina [31], Mazziotti [32], Greenman and Mazziotti [33]. They started from the Schrödinger equation in the matrix form

$$\langle \widehat{A}\,\widehat{H}\,\widehat{Q}_\alpha\rangle = E_\alpha\langle \widehat{A}\,\widehat{Q}_\alpha\rangle. \tag{4}$$

If m-particle excitations are included in $\widehat{Q}_\alpha$, the $(2m+2)$-RDMs are obviously needed, however, by using a commutator, one excitation operator can be eliminated. In the case of single excitations, it leads to a theory that can be formulated in terms of 3-RDMs. This is a big computational saving. Additionally one can use the cumulant method to approximately reconstruct 3-RDM from the 2-RDM, or take advantage of the semidefinite programming for a more efficient construction of the density matrices [33].

Thus, there are two classes of methods for the determination of excited states that make use of the 2-RDM, either through Eq. (1) provided that the consistency condition holds, or from Eq. (3) by neglecting the connected reduced density matrix (cRDM) ${}^3\Delta$. However, there is even a more direct connection between the EOM and the EKT methods that will be established here. It is based on the idea that every excitation in many-body systems can be represented as a superposition of simpler ones. For instance, neutral excitations can be regarded as transitions between the quasiparticle states, which include self-energy corrections, or doubly excited states can be described in a basis of singly excited states. It is then shown that the residual interactions between such configurations are described by the effective EOM Hamiltonian involving two commutators as in Eq. (1). Building upon this theoretical insight, excited-state calculations can be performed without relying upon the consistency condition or neglecting the higher-order cRDMs.

Besides establishing this important finding in Sec. IV, a number of supporting results are presented. In Sec. II A, we specialize Eq. (3) for the cases of single and double excitations. Very compact and transparent notations are proposed. In Sec. II B, we specialize Eq. (1) for the case of single excitations from a correlated ground state. This serves the purpose of directly comparing the EOM (1) and the EKT (3) approaches. As the underlying assumption, we consistently neglect the connected density matrices ${}^3\Delta$ and ${}^2\Delta$. It is shown that resulting equations are not identical, but can be reduced to the same form for the idempotent 1-RDM. From the numerical perspective, Eqs. (1) and (3) are very similar: they represent a generalized eigenvalue problem, which is also pertinent to the Casida equation [47] (Meer *et al.* [48] compare the form of this equation for different scenarios). For a completely exact or a completely uncorrelated ground state the metric (the matrix on the right-hand side) is symmetric and positive definite. For approximate states, these two conditions may not be fulfilled. Thus, some dedicated methods need to be developed. A stable and universal solution based on the singular value decomposition (SVD) is proposed in Sec. II C. In Sec. III we present numerical calculations (corresponding data is tabulated in Appendix for the stretched water molecule, which develops singlet-triplet instability far from the equilibrium geometry. We demonstrate that Eq. (3) yields very accurate energies by including only single excitations. This is not possible to achieve with ERPA—double excitations are needed. Another important message of this section is the excellent descriptions (even of quintet states) that were obtained by including double excitations in Eq. (3). The calculations are numerically very demanding because 5-RDMs are needed.

II. THEORY

A. Explicit forms of Eq. (3)

A general excitation operator $\widehat{Q}_\alpha^{(m,n)}$ adds m electrons to the system and consists of n fermionic creation $\psi^\dagger(\mathbf{x})$ or annihilation operators $\psi(\mathbf{x})$:

$$\widehat{Q}_\alpha^{(m,n)} = \int d(\mathbf{x}_1 \ldots \mathbf{x}_p) \int d(\mathbf{y}_1 \ldots \mathbf{y}_q)\, w_\alpha(\mathbf{x}_1 \ldots \mathbf{x}_p; \mathbf{y}_1 \ldots \mathbf{y}_q) \times \hat{\psi}^\dagger(\mathbf{x}_1)\cdots\hat{\psi}^\dagger(\mathbf{x}_p)\hat{\psi}(\mathbf{y}_1)\cdots\hat{\psi}(\mathbf{y}_q), \tag{5}$$

where $p+q=n$ and $p-q=m$, and vector $\mathbf{x}_i \equiv (\mathbf{r}_i, \sigma_i)$ is a shorthand for composite position and spin variables. It is sufficient to consider the normal operator order. In the original EKT $n=1$ and $m=\pm 1$. The generalized ansatz as in

Eq. (5) was discussed by Ayers and Melin [49]. The n-particle Dyson orbitals $w_\alpha(\mathbf{x}_1 \ldots \mathbf{x}_n)$ in the expansion of the excitation operators are determined from the requirement that $|\Psi_\alpha^{(m)}\rangle$ are the eigenstates of the full Hamiltonian:

$$\widehat{H} = \iint d(\mathbf{xy}) \Big[\hat{\psi}^\dagger(\mathbf{x}) t(\mathbf{x},\mathbf{y}) \hat{\psi}(\mathbf{y}) + \frac{1}{2} \hat{\psi}^\dagger(\mathbf{x}) \hat{\psi}^\dagger(\mathbf{y}) v(\mathbf{x},\mathbf{y}) \hat{\psi}(\mathbf{y}) \hat{\psi}(\mathbf{x}) \Big], \tag{6}$$

where $t(\mathbf{x},\mathbf{y})$ and $v(\mathbf{x},\mathbf{y})$ are one- and two-body operators. We denote corresponding energies as $E_\alpha^{(m)}$ and notice that the excitation energies $\epsilon_\alpha^{(m)} = E_\alpha^{(m)} - E_0$ can be expressed in terms of the commutator of the excitation operator with the Hamiltonian.

$$\big\langle \widehat{A} \big[\widehat{H}, \widehat{Q}_\alpha^{(m,n)} \big] \big\rangle = \epsilon_\alpha^{(m)} \big\langle \widehat{A}\, \widehat{Q}_\alpha^{(m,n)} \big\rangle. \tag{7}$$

Notice that no approximations are involved in the derivation of Eq. (7). However, it is important that a set of auxiliary operators $\widehat{A}$ is big enough so that w_α can be determined. Equation (7) has a structure of the extended Koopmans theorem, which will be referred to as EKT-n, where n stands for the total number of creation and annihilation operators as defined by Eq. (5).

We will work now in a finite basis of real functions ($\{\phi_i(\mathbf{r})\}$, $i = 1, \ldots, N_b$), and introduce the associated creation and annihilation operators:

$$\hat{\psi}(\mathbf{x}) = \sum_i \phi_i(\mathbf{r}) \hat{c}_{j\sigma}, \quad \hat{\psi}^\dagger(\mathbf{x}) = \sum_i \phi_i(\mathbf{r}) \hat{c}_{j\sigma}^\dagger. \tag{8}$$

The many-body Hamiltonian can be expressed in terms of the excitation operators $\widehat{E}_{ij}^\sigma = \hat{c}_{i\sigma}^\dagger \hat{c}_{j\sigma}$ and $\widehat{E}_{ij} = \widehat{E}_{ij}^\alpha + \widehat{E}_{ij}^\beta$, where α, β stand for spin-up, -down contributions, respectively:

$$\widehat{H} = \sum_{ab} t_{ab} \widehat{E}_{ab} + \frac{1}{2} \sum_{ab,cd} (ab|cd)(\widehat{E}_{ab}\widehat{E}_{cd} - \delta_{bc}\widehat{E}_{ad}).$$

Here, the one-body matrix elements are defined as $t_{ab} = \int d\mathbf{r} \phi_a^*(\mathbf{r}) \hat{t}(\mathbf{r}) \phi_b(\mathbf{r})$, and for the Coulomb integrals we use the chemistry notation to emphasize the eightfold permutation symmetry $(ab|cd) = \iint d(\mathbf{r},\mathbf{r}') \phi_a^*(\mathbf{r}) \phi_b(\mathbf{r}) v(\mathbf{r} - \mathbf{r}') \phi_c^*(\mathbf{r}') \phi_d(\mathbf{r}')$. We introduce now a set of effective Fock operators $\widehat{F}_{ij}$ and express the commutators of $\widehat{H}$ with the excitation operators $\widehat{E}_{ij}^\sigma$ in their terms:

$$\widehat{F}_{ij} = t_{ij} + \sum_{cd} \widehat{E}_{cd} (cd|ij), \tag{9}$$

$$\partial \widehat{E}_{ij}^\sigma = \big[\widehat{H}, \widehat{E}_{ij}^\sigma \big] = \sum_a \widehat{E}_{aj}^\sigma \widehat{F}_{ai} - \sum_b \widehat{F}_{jb} \widehat{E}_{ib}^\sigma, \tag{10}$$

Notice that indices a, b and i, j do not have a special meaning of occupied or virtual states, as is sometimes adopted in quantum chemistry [50]. The differential operator ∂ fulfills the standard product rule $\partial(\hat{X}\hat{Y}) = \hat{X}(\partial\hat{Y}) + (\partial\hat{X})\hat{Y}$.

Neutral excited states can be computed by specializing Eq. (7) for $n = 2$, 4. They can be written in a very transparent form if the collection of the orbital and spin indices is denoted by one vector index $\hat{X}_{ij}^\sigma \equiv \hat{X}_{\boldsymbol{\xi}}$ and the Einstein summation over the repeated ones is assumed. In these notations the considered excitation operators are

$$\widehat{Q}_\alpha^{(0,2)} = \widehat{E}_{\boldsymbol{\mu}} w_{\boldsymbol{\mu},\alpha}, \quad \widehat{Q}_\alpha^{(0,4)} = \widehat{E}_{\boldsymbol{\mu}} \widehat{E}_{\boldsymbol{\nu}} w_{\boldsymbol{\mu\nu},\alpha}. \tag{11}$$

By selecting $\widehat{A}$ to comprise single, double excitations, respectively, we arrive at the eigenvalue equations determining excited states:

$$\langle \widehat{E}_{\boldsymbol{\zeta}}\, \partial \widehat{E}_{\boldsymbol{\mu}} \rangle w_{\boldsymbol{\mu},\alpha} = \epsilon_\alpha^{(0)} \langle \widehat{E}_{\boldsymbol{\zeta}}\, \widehat{E}_{\boldsymbol{\mu}} \rangle w_{\boldsymbol{\mu},\alpha}, \tag{12a}$$

$$\langle \widehat{E}_{\boldsymbol{\zeta}} \widehat{E}_{\boldsymbol{\eta}}\, \partial(\widehat{E}_{\boldsymbol{\mu}} \widehat{E}_{\boldsymbol{\nu}}) \rangle w_{\boldsymbol{\mu\nu},\alpha} = \epsilon_\alpha^{(0)} \langle \widehat{E}_{\boldsymbol{\zeta}} \widehat{E}_{\boldsymbol{\eta}}\, \widehat{E}_{\boldsymbol{\mu}} \widehat{E}_{\boldsymbol{\nu}} \rangle w_{\boldsymbol{\mu\nu},\alpha}. \tag{12b}$$

The ground-state correlators $\langle \widehat{E}_{\boldsymbol{\zeta}} \ldots \widehat{E}_{\boldsymbol{\nu}} \rangle$ can be expressed in terms of the reduced density matrices [51]:

$${}^p D_{j_1 j_2 \ldots j_p}^{i_1 i_2 \ldots i_p} = \frac{1}{p!} \big\langle c_{i_1}^\dagger c_{i_2}^\dagger \cdots c_{i_p}^\dagger c_{j_p} c_{i_{p-1}} \cdots c_{j_1} \big\rangle. \tag{13}$$

Therefore, we have

$$\big\langle \widehat{E}_{ax}^\alpha \big\rangle = {}^1D_x^a, \tag{14a}$$

$$\big\langle \widehat{E}_{ax}^\alpha \widehat{E}_{by}^\alpha \big\rangle = 2!\, {}^2D_{xy}^{ab} + \delta_{bx}\, {}^1D_y^a. \tag{14b}$$

$$\big\langle \widehat{E}_{ax}^\alpha \widehat{E}_{by}^\alpha \widehat{E}_{cz}^\alpha \big\rangle = 3!\, {}^3D_{xyz}^{abc} - 2!\, \delta_{cy}\, {}^2D_{zx}^{ab} + 2!\, \delta_{cx}\, {}^2D_{zy}^{ab} - 2!\, \delta_{bx}\, {}^2D_{zy}^{ac} + \delta_{bx}\delta_{c,y}\, {}^1D_z^a. \tag{14c}$$

Only spin-up (α) components are shown. Other spin components and higher correlators can be expressed similarly using the anticommutation relations for creation and annihilation operators.

The computational complexity of equations (12) is set by the dimension of the variational space $N_v = O(N_b^n)$: we find that the brute-force solution of the EKT-4 equation is only feasible for a maximum of $N_b = 10$ basis functions.[1]

The generalization of Eqs. (12) to higher-order excitations is obvious. However, let us return to the original extended Koopmans theorem for ionization potentials (IPs) and electron affinities (EAs):

$$\langle \hat{c}_{i\sigma'}^\dagger [\widehat{H}, \hat{c}_{j\sigma}] \rangle x_{j\sigma,\alpha} = \epsilon_\alpha^{(-)} \langle \hat{c}_{i\sigma'}^\dagger \hat{c}_{j\sigma} \rangle x_{j\sigma,\alpha}, \tag{15a}$$

$$\langle \hat{c}_{j\sigma'} [\widehat{H}, \hat{c}_{i\sigma}^\dagger] \rangle y_{i\sigma,\alpha} = \epsilon_\alpha^{(+)} \langle \hat{c}_{j\sigma'} \hat{c}_{i\sigma}^\dagger \rangle y_{i\sigma,\alpha}, \tag{15b}$$

and present a useful generalization, which differs by the choice of the operators $\widehat{A}$:

$$\langle \widehat{E}_{\boldsymbol{\zeta}} \hat{c}_{i\sigma'}^\dagger [\widehat{H}, \hat{c}_{j\sigma}] \rangle x_{j\sigma,\alpha} = \epsilon_\alpha^{(-)} \langle \widehat{E}_{\boldsymbol{\zeta}} \hat{c}_{i\sigma'}^\dagger \hat{c}_{j\sigma} \rangle x_{j\sigma,\alpha}, \tag{16a}$$

$$\langle \widehat{E}_{\boldsymbol{\zeta}} \hat{c}_{j\sigma'} [\widehat{H}, \hat{c}_{i\sigma}^\dagger] \rangle y_{i\sigma,\alpha} = \epsilon_\alpha^{(+)} \langle \widehat{E}_{\boldsymbol{\zeta}} \hat{c}_{j\sigma'} \hat{c}_{i\sigma}^\dagger \rangle y_{i\sigma,\alpha}. \tag{16b}$$

Notice that these equations are intermediate between the simplest EKT-1 (15) and the EKT-3 equations, which were studied by Farnum *et al.* [52].

Terminology. Equations (12), (15), (16) are analyzed in detail below. The variational space of the first group of equations, i.e., EKT-2 ($n = 2$) and EKT-4 ($n = 4$) is comparable

[1]The brute-force approach can be made more efficient by the elimination of the linear dependence in excitation operators and the spin adaptation. The bottleneck is not as much the solution of these equations, but rather the construction and the storage of the correlators.

to that of the configuration interaction methods with single and double excitations, CIS and CISD, respectively. Equations from the second group ($n = 1$) represent the extended Koopmans theorem in the original formulation [30].

B. EKT vs EOM

The two theories can be directly compared in some limiting cases. Following Mazziotti [53], the connected p-reduced density matrices (p-cRDMs) are introduced. The lowest-order RDMs can be expressed as follows:

$$^1D = {}^1\Delta, \tag{17a}$$

$$^2D = {}^2\Delta + {}^1\Delta \wedge {}^1\Delta, \tag{17b}$$

$$^3D = {}^3\Delta + {}^1\Delta \wedge {}^1\Delta \wedge {}^1\Delta + 3\,{}^2\Delta \wedge {}^1\Delta, \tag{17c}$$

where $\wedge$ is the wedge product of two tensors. Let us now explicitly evaluate Eq. (12a) assuming

$$^3\Delta = {}^2\Delta = 0, \quad {}^1\Delta_{ij} = {}^1D_{ij} = n_i\delta_{ij}. \tag{18}$$

The natural orbital basis is adopted here. In this basis the 1-RDM is diagonal. We introduce for brevity the hole population $h_i = 1 - n_i$, which is complementary to the particle population, and denote $\bar\sigma$ the spin projection opposite to σ. Calculations are performed analytically using *Mathematica* computer algebra system. They yield:

$$\begin{aligned}\langle \widehat{E}^\sigma_{kl}\,\partial\,\widehat{E}^\sigma_{ij}\rangle_0 &= n_k\delta_{kl}(n_j - n_i)\epsilon_{ji} + n_k h_l(\delta_{jk}\epsilon_{li} - \delta_{li}\epsilon_{jk}) \\ &\quad + n_k h_l(n_j - n_i)(lk||ji),\end{aligned} \tag{19a}$$

$$\begin{aligned}\langle \widehat{E}^{\bar\sigma}_{kl}\,\partial\,\widehat{E}^\sigma_{ij}\rangle_0 &= n_k\delta_{kl}(n_j - n_i)\epsilon_{ij} \\ &\quad + n_k h_l(n_j - n_i)(lk|ji),\end{aligned} \tag{19b}$$

$$\langle \widehat{E}^\sigma_{kl}\,\widehat{E}^\sigma_{ij}\rangle_0 = n_k n_i\delta_{kl}\delta_{ij} + n_k h_l\delta_{jk}\delta_{li}, \tag{19c}$$

$$\langle \widehat{E}^{\bar\sigma}_{kl}\,\widehat{E}^\sigma_{ij}\rangle_0 = n_k n_i\delta_{kl}\delta_{ij}. \tag{19d}$$

Similar calculations for the EOM approach can be found in, e. g., Chatterjee and Pernal [35]. They read:

$$\begin{aligned}\langle [\widehat{E}^\sigma_{kl},\,\partial\,\widehat{E}^\sigma_{ij}]\rangle_0 &= (n_k - n_l)(\delta_{jk}\epsilon_{li} - \delta_{li}\epsilon_{jk}) \\ &\quad + (n_k - n_l)(n_j - n_i)(lk||ji),\end{aligned} \tag{20a}$$

$$\langle [\widehat{E}^{\bar\sigma}_{kl},\,\partial\,\widehat{E}^\sigma_{ij}]\rangle_0 = (n_k - n_l)(n_j - n_i)(lk|ji), \tag{20b}$$

$$\langle [\widehat{E}^\sigma_{kl},\,\widehat{E}^\sigma_{ij}]\rangle_0 = (n_k - n_l)\delta_{li}\delta_{jk}, \tag{20c}$$

$$\langle [\widehat{E}^{\bar\sigma}_{kl},\,\widehat{E}^\sigma_{ij}]\rangle_0 = 0. \tag{20d}$$

Here, we additionally introduced the effective Hartree-Fock Hamiltonian

$$\epsilon_{jk} = h_{jk} + \sum_c 2n_c(cc|jk) - \sum_c n_c(ck|jc), \tag{21}$$

and the antisymmetrized Coulomb matrix elements:

$$(lk||ji) = (lk|ji) - (li|jk). \tag{22}$$

Equations (19) and (20) are in general not equivalent. Provided the ground-state occupation numbers n_i are known from some correlated calculations, it is tempting to use them as a refinement for the ordinary RPA. According to Chatterjee and Pernal [35] "using correlated 1-RDM's in the linearized ERPA equations does not bring improvement over RPA." We arrived at the same conclusion starting from Eq. (19). The reason is that the connected RDMs are expected to be lower in magnitude than the disconnected components only for separable noninteracting subsystems (Ref. [51], chap. 10). For systems where all pairwise interactions are present, they need not be small.

For a single-determinant ground state, the 1-RDM is idempotent and the effective Hamiltonian (21) is diagonal, $\epsilon_{jk} = \epsilon_j\delta_{jk}$. Therefore, the first terms of Eqs. (19a), (19b) vanish due to $(n_j - n_i)\epsilon_{ij} = 0$. Adopting a standard enumeration of rows [composite (ij) index] and columns (lk), the metric takes a symmetric matrix form because (i) $\delta_{jk}\delta_{li}$ is a diagonal matrix; and (ii) $n_j n_l\delta_{kl}\delta_{ij} = n_i n_k\delta_{kl}\delta_{ij}$. The Hamiltonian matrix is not symmetric due to the terms containing Coulomb interaction. However, the EKT-2 equation reduces to the RPA equation by subtracting the two equations with interchanged k and l indices and considering that $n_k h_l - n_l h_k = n_k - n_l$.

From Eqs. (20) and (19), it is evident that the overlap matrix is rank deficient for uncorrelated reference states. For weakly correlated states, there are many small eigenvalues. They need to be eliminated as discussed below.

C. Numerical approach

Equations (12) belong to the class of generalized eigenvalue problems $\mathbf{F}\mathbf{w}_\alpha = \epsilon_\alpha\mathbf{S}\mathbf{w}_\alpha$. In analogy with electronic structure methods, we designate $\mathbf{F}$ as the generalized Fock and $\mathbf{S}$ as the overlap matrices. They can be indexed in such a way that for the exact RDMs the matrix $\mathbf{F}$ is symmetric, whereas $\mathbf{S}$ is symmetric and positive definite. For approximate densities these properties cannot be warranted (as was also observed for EKT [41]). In the eigenvalue problem (16), the matrices are not even square. Thus, specialized methods are required. We found the following stable procedure that works for nonexact densities. On the first and computationally most demanding step a singular value decomposition of the overlap is performed $\mathbf{S} = \mathbf{U}\mathbf{\Sigma}\mathbf{V}^T$, where $\mathbf{U}^T\mathbf{U} = \mathbf{V}^T\mathbf{V} = \mathbf{I}$ are orthogonal matrices, and $\mathbf{\Sigma} = \mathrm{diag}(\sigma_1 \geqslant \sigma_2 \geqslant \ldots \geqslant \sigma_{N_v})$ is real and diagonal. Dominant eigenvalues of the overlap (above a certain threshold, $\{\sigma_i > T_{\mathrm{SVD}}\}$, $1 \leqslant i \leqslant N_t < N_v$) are selected and the effective Fock matrix is built and diagonalized; subsequently, the found eigenvectors are back-transformed:

$$\widetilde{F}_{ij} = \frac{\mathbf{u}_i^T}{\sqrt{\sigma_i}}\mathbf{F}\frac{\mathbf{v}_j}{\sqrt{\sigma_j}}, \quad \widetilde{\mathbf{F}}\tilde{\mathbf{w}}_\alpha = \epsilon_\alpha\tilde{\mathbf{w}}_\alpha, \quad \mathbf{w}_\alpha = \sum_{i=1}^{k}\frac{\tilde{w}_{i\alpha}}{\sqrt{\sigma_i}}\mathbf{v}_i.$$

Typically the number of eigenvalues of the overlap above the threshold $N_t \ll N_v$ because the full set of excitation operators (11) is not linearly independent.

Besides energies, the spectral strength is an important characteristic of excited states. Assuming that vectors $\mathbf{w}_\alpha$ are normalized according to

$$\mathbf{w}_\alpha^T\mathbf{S}\mathbf{w}_\alpha = \mathbf{I}, \tag{23}$$

it can be computed as follows:

$$z_\alpha = \sum_{\boldsymbol{\kappa}} |\langle \widehat{E}_{\boldsymbol{\kappa}}\widehat{E}_{\boldsymbol{\mu}}\rangle w_{\boldsymbol{\mu},\alpha}|^2, \quad z_\alpha = \sum_{\boldsymbol{\kappa}} |\langle \widehat{E}_{\boldsymbol{\kappa}}\widehat{E}_{\boldsymbol{\mu}}\widehat{E}_{\boldsymbol{\nu}}\rangle w_{\boldsymbol{\mu\nu},\alpha}|^2.$$

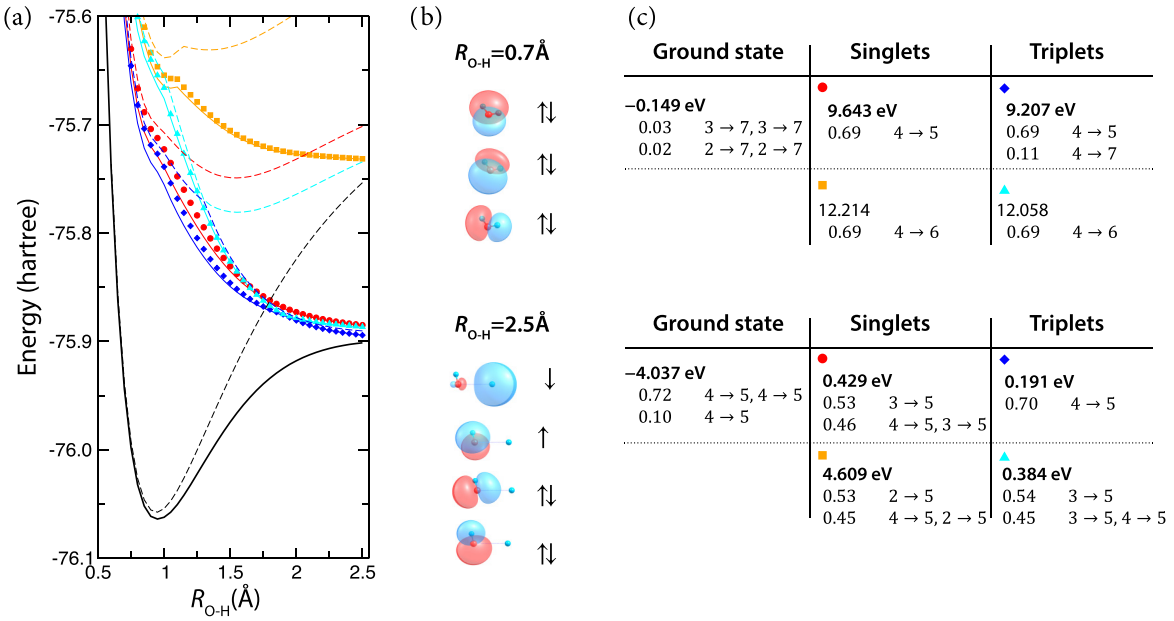

FIG. 1. (a) Potential energy surfaces of H_2O at the experimental values of the H(1)-O-H(2) angle (104.45°) and the O-H(1) distance (0.9484 Å) as functions of the O-H(2) bond length. Results of the calculation on the (6,6) subspace by exact diagonalization (full lines) and EKT-2 with $T_{SVD} = 10^{-3}$ (dots) are compared with CIS (dashed lines) using a consistent color coding. The ground reference state is shown in black, singlet excitations—in red and orange, triplet excitations—in blue and cyan. (b) Natural molecular orbitals of the ground state for two O-H(2) bond lengths. (c) Summary of the EOM-CCSD calculations: energies in eV (with respect to RHF value for the ground state, and with respect to CCSD value for excited states, first line) and weight of dominant electron configurations (second and third line) are shown for each state for $R_{O\text{-}H(2)} = 0.7$ Å (top) and $R_{O\text{-}H(2)} = 2.5$ Å (bottom).

III. NUMERICAL VALIDATION

In this section we study the performance of EKT-2 and EKT-4 methods using correlated ground-state RDMs. As is evident from Eqs. (12), 2- and 3-RDMs are required for the EKT-2 approach and 4- and 5-RDMs are needed for the EKT-4 approach. Unless explicitly indicated, these RDMs are evaluated from the ground-state wave function obtained from the exact diagonalization of the many-body Hamiltonian without using any further approximations.

To illustrate the procedure, we study the single-bond breaking in a water molecule. This is a commonly used benchmarking scenario because electronic correlations can be tuned by stretching the bond from the equilibrium distance (where the wave function is dominated by a single Slater determinant) to a more correlated multideterminant case [54–56]. Such electronic states cannot be treated on the basis of adiabatic TDDFT [37,57,58] or configuration interaction singles (CIS). In Fig. 1(a) the energies of two lowest singlet and triplet excitations are plotted as a function of the $R_{O\text{-}H(2)}$ bond distance for a fixed angle (the experimental value of 104.45°).[2] We use the cc-pVTZ basis set and perform calculations on the active space comprising six electrons in six orbitals using our own implementation for integrals [59] and the graphical unitary group approach [60,61] for the configuration interaction [54]. Supporting calculations within the equation of motion coupled cluster approach (EOM-CCSD) and the restricted Hartree-Fock (RHF) reference, provide insight on the nature of the electronic states. At short distances the ground electronic state is weakly correlated, the singlet and triplet excited states are of single excitation character. Stretching one of the bonds, the closed-shell solution becomes unstable at 1.7 Å, which is manifested as negative singlet-triplet CIS excitation energy. For larger distances, an open-shell singlet ground state is favored with approximate electronic configuration depicted on Fig. 1(b). In order to describe such a state on the basis of RHF, simultaneous promotion of the spin-up and spin-down electrons from HOMO to LUMO is needed. This is a double excitation with a weight 0.72 as shown in Fig. 1(c). The lowest triplet excitation is of very similar nature, therefore it can be regarded as single excitation. In contrast, other excited states are correlated: in order to restore a physically correct picture in the dissociative limit, very large corrections of the CIS values are needed, which is accomplished by our EKT-2 approach by including interactions between the virtual orbitals. They are absent in the EOM approach.

The EKT-2 approach is also very economical in terms of the size of variational space.[3] In our next calculation, we

[2]We further notice that there is a conical intersection of two lowest singlet states at almost linear geometry: exact calculations predict a crossing of the two energy surfaces for a specific bond length in the linear geometry, whereas in CIS or adiabatic TDDFT a one-dimensional seam is formed for a range of the H(1)-O-H(2) angles [57].

[3]For the considered system in (6,6) active space and $T_{SVD} = 10^{-2}$ cutoff, at most 28 amplitudes must be optimized, in contrast to 153 amplitudes in the unrestricted EOM-CCSD approach.

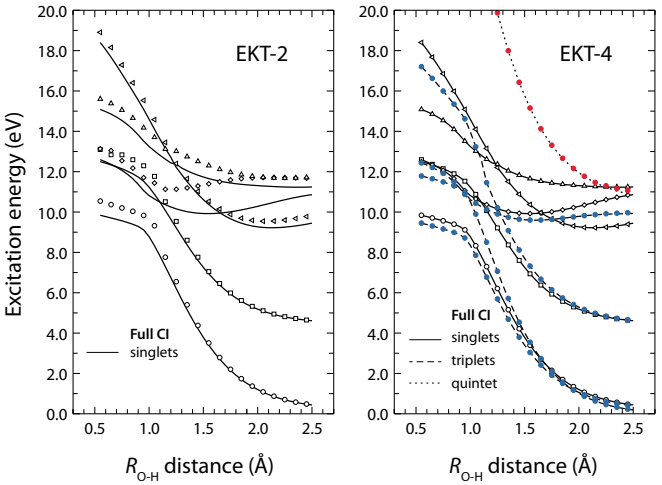

FIG. 2. Potential energy surfaces of the H_2O molecule as a function of $R_{O\text{-}H(1)}$ at EKT-2 (left) and EKT-4 (right) levels of theory using $T_{SVD} = 10^{-2}$ cutoff are compared with the full CI calculations. Notice that correct spin symmetry is obtained even without the spin adaptation prior to the diagonalization. Rather large cutoff was used to demonstrate that EKT is a very economical theory in terms of the size of variational space.

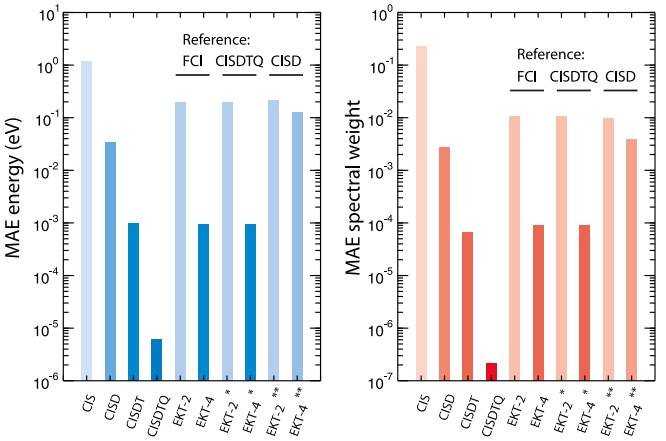

FIG. 3. Mean absolute errors of the excitation energy (left) and spin resolved spectral weight (right) of the first singlet excited state for a number of methods. $T_{SVD} = 10^{-3}$ cutoff is used for all EKT calculations. The accuracy of CIS is reduced due to the presence of the singlet-triplet instability. Providing correct ordering of excited states, the generalized Koopmans theorem yields almost an order of magnitude improvement over its CI counterparts. However, the errors crucially depend on the reference state: using CISD density reduces the accuracy of the EKT-4, whereas CISDTQ does not.

deliberately use a rather high $T_{SVD} = 10^{-2}$ cutoff, which adds just a few virtual-virtual transitions. Nonetheless, energies of other excited singlets (Fig. 2, left) and triplets are well reproduced. As expected, for a weakly correlated ground state (close to the equilibrium geometry) the EKT-2 solution is less accurate collapsing onto the CIS energies (visible as a discontinuity in EKT-2 results at $R_{O\text{-}H(2)} = 1.1$ Å in Fig. 2, left). This can be cured by either reducing the cutoff or by going to the next level of theory (EKT-4, Fig. 2, right), which also gives access to quintet states. In fact, EKT-2 and EKT-4 are almost one order of magnitude more accurate than corresponding CIS and CISD methods. This conclusion holds for the mean absolute error (MAE) of the energy as well as of the oscillator strength (Fig. 3). Here, we define the MAE of a quantity f as a sum over N geometrical configurations

$$\mathrm{MAE} = \frac{1}{N}\sum_{i=1}^{N} \left| f_i^{\mathrm{c}} - f_i^{\mathrm{r}} \right|, \tag{24}$$

where f_i^{c} and f_i^{r} refer to the computed and the reference values, respectively.

In Fig. 4 we compare the performance of the EKT-2 vs. EOM. Exact RDMs is used for EKT-2, whereas exact and noninteracting RDMs are used for the equation of motion. The EOM approach is significantly less accurate, this is manifest most of all in the oscillator strength, which reaches unphysical values above 1. However, it is known that the Thomas-Reiche-Kuhn sum rule is satisfied [62]. We also observe that some triplet states cannot be found (i.e., EOM approach yields solutions that are significantly different from the exact ones, so that a correspondence between both methods cannot be established) for stretched geometries ($R_{O\text{-}H}$ above 1.4 Å for uncorrelated reference state and above 1.8 Å for fully correlated reference). In approaching the point of single-triplet instability, the spectral strength becomes very large. It has been suggested that some of the deficiencies of the EOM approach can be cured by explicitly adding double excitations [35,37]. We do not add these excitations here for a fair comparison with the EKT-2 method. A clear conclusion at this point is that EKT-2 can accurately predict the single-triplet instability, whereas EOM not. Since the only difference between the methods is that the consistency relation (2) is not needed in the EKT approach, we will explore this point in detail now.

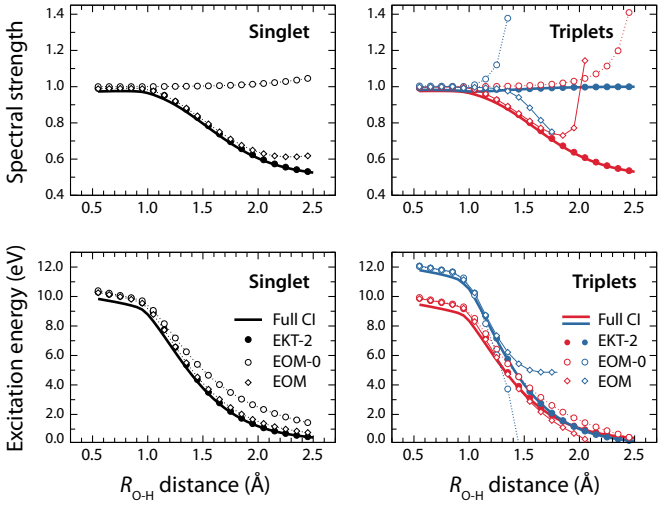

FIG. 4. Spectral strength and energies of the lowest singlet (left) and two triplets states (right) of the H_2O molecule as a function of $R_{O\text{-}H(1)}$ at the full CI, EKT-2, and EOM levels of theory (EOM-0 refer to uncorrelated reference states).

IV. EKT FOR COMPOSITE EXCITATIONS

Despite the deficiencies mentioned above, the equation of motion approach is a very convenient starting point for the treatment of correlated excited states. It is well known that for single-determinant states (Hartree-Fock or Kohn-Sham) and for single excitations it reduces to the random phase approximation or adiabatic TDDFT, respectively [62]. Higher excitations can readily be incorporated into the effective Hamiltonian. However, they are typically treated perturbatively by down-folding the Hamiltonian onto the space of single excitations [36–38]. Such effective Hamiltonian can be analyzed diagrammatically by building parallels with the Bethe-Salpeter equation. According to Sangalli *et al.* [23], the diagrams do not include the self-energy corrections. This is clearly related to the violation of the consistency condition (2). Numerical calculations above (Fig. 4) demonstrate that self-energy corrections are essential and are indeed present in the EKT approach, which does not rely on the consistency condition. In fact, one can demonstrate explicitly that EKT equations for neutral excitations contain self-energy corrections.

It is often instructive to think about complex excitations in many-body systems as being composed of simpler ones. Many-body perturbation theory gives, for instance, a prescription how the propagator describing a particle-hole pair can be represented in terms of the diagrams with single-particle propagators as building blocks. Something similar can be achieved starting from the basic EKT equation (3). Let us expand the excitation operator $\widehat{Q}_\gamma$ in direct products of simpler excitations:

$$\widehat{Q}^{(C)}_\gamma = \sum_{\alpha\beta} C_{\alpha\beta,\gamma}\, \widehat{Q}^{(A)}_\alpha \widehat{Q}^{(B)}_\beta, \tag{25}$$

where we demand that the total number of electrons added to the system is $m_C = m_A + m_B$, and that $\widehat{Q}^{(C)}_\gamma$ consists of $n_C = n_A + n_B$ fermionic creation or annihilation operators, viz., definition (5). The EKT equation can be reformulated by using these two commutator identities:

$$\begin{aligned}\big[\widehat{H}, \widehat{Q}^{(A)}_\alpha \widehat{Q}^{(B)}_\beta\big] &= \widehat{Q}^{(A)}_\alpha \big[\widehat{H}, \widehat{Q}^{(B)}_\beta\big] + \widehat{Q}^{(B)}_\beta \big[\widehat{H}, \widehat{Q}^{(A)}_\alpha\big] \\ &\quad - \big[\widehat{Q}^{(B)}_\beta, \big[\widehat{H}, \widehat{Q}^{(A)}_\alpha\big]\big] \qquad (26a)\\ &= \widehat{Q}^{(A)}_\alpha \big[\widehat{H}, \widehat{Q}^{(B)}_\beta\big] - \widehat{Q}^{(B)}_\beta \big[\widehat{H}, \widehat{Q}^{(A)}_\alpha\big] \\ &\quad + \big\{\widehat{Q}^{(B)}_\beta, \big[\widehat{H}, \widehat{Q}^{(A)}_\alpha\big]\big\}, \qquad (26b)\end{aligned}$$

where $\{\widehat{A}, \widehat{B}\} \equiv \widehat{A}\widehat{B} + \widehat{B}\widehat{A}$ denotes an anticommutator. In the former, latter identities should be used for bosoniclike, fermioniclike excitations, respectively. Now the crucial observation allowing to simplify the resulting EKT equations is that

$$\big\langle \widehat{A}\big[\widehat{H}, \widehat{Q}^{(A/B)}_{\alpha/\beta}\big]\big\rangle = (E_{\alpha/\beta} - E_0)\big\langle \widehat{A}\widehat{Q}^{(A/B)}_{\alpha/\beta}\big\rangle \tag{27}$$

holds for any choice of auxiliary operators $\widehat{A}$ provided that $\widehat{Q}^{(A/B)}_{\alpha/\beta}|\Psi_0\rangle$ are exact eigenstates. Equations (15), (16) illustrate, for instance, how quasiparticle (-hole) excitations can be obtained either from the equations involving either 2-RDMs or 3-RDMS, respectively. When $\widehat{Q}^{(A)}_\alpha$, $\widehat{Q}^{(B)}_\beta$ are only approximations for the true excitation operators, Eq. (27) may not hold for an arbitrary $\widehat{A}$. Nonetheless, this assumption is a reasonable starting point for the derivation of simplified theories bases on EKT. In combination with the fact that an additional (anti)commutator reduces the number of excitation operators by one, the correlators arising from the right-hand side of Eqs. (26) are simpler than the correlator arising from the respective left-hand side. The physical content of this approximation is that by neglecting interactions between the A and B excitations, the excitation energies are approximately given by

$$\epsilon^{(m_C)}_\gamma \approx \epsilon^{(m_A)}_\alpha + \epsilon^{(m_B)}_\beta, \tag{28}$$

and

$$\widehat{\mathcal{H}}^{\pm}_{\alpha\beta} = \pm\big[\widehat{Q}^{(B)}_\beta, \big[\widehat{H}, \widehat{Q}^{(A)}_\alpha\big]\big]_\pm \mp \epsilon_\alpha \big[\widehat{Q}^{(B)}_\beta, \widehat{Q}^{(A)}_\alpha\big]_\pm \tag{29}$$

are effective Hamiltonians describing interactions between these excitations. Here, we denote for brevity commutators as $[\ldots]_-$, and anticommutators as $[\ldots]_+$. Equation (29) has obviously the form of the EOM effective Hamiltonian (1).

In summary, the EKT for the $\widehat{Q}^{(C)}_\gamma$ excitations can be written by virtue of the identities (26) as a generalized eigenvalue problem:

$$\begin{aligned}\sum_{\alpha\beta} \langle \widehat{A}\widehat{\mathcal{H}}^{\pm}_{\alpha\beta}\rangle C_{\alpha\beta,\gamma} &= \big(\epsilon^{(m_C)}_\gamma - \epsilon^{(m_A)}_\alpha - \epsilon^{(m_B)}_\beta\big) \\ &\quad \times \sum_{\alpha\beta} \big\langle \widehat{A}\widehat{Q}^{(A)}_\alpha \widehat{Q}^{(B)}_\beta\big\rangle C_{\alpha\beta,\gamma}, \qquad (30)\end{aligned}$$

with the equation-of-motion Hamiltonian (29) in the basis of excitations $\widehat{Q}^{(A)}_\alpha$ and $\widehat{Q}^{(B)}_\beta$ that are given as the solutions of simpler EKT eigenproblems (27).

We will now consider two examples for the neutral excitations given by Eqs. (11):

(*a*) $\widehat{Q}^{(A)}_\alpha \equiv \widehat{Q}^{(1,1)}_\alpha$, $\widehat{Q}^{(B)}_\beta \equiv \widehat{Q}^{(-1,1)}_\beta$ forming $\widehat{Q}^{(C)}_\gamma \equiv \widehat{Q}^{(0,2)}$;

(*b*) $\widehat{Q}^{(A)}_\alpha \equiv \widehat{Q}^{(0,2)}_\alpha$, $\widehat{Q}^{(B)}_\beta \equiv \widehat{Q}^{(0,2)}_\beta$ forming $\widehat{Q}^{(C)}_\gamma \equiv \widehat{Q}^{(0,4)}$.

The method is, however, not limited to neutral excitations, but can be used to derive effective Hamiltonians for charged excitations such as trions [63], albeit without screening, or for photoemitted electrons in continuum [64], and is similar in spirit to recent results of Yang *et al.* [18].

a. Neutral excitations as 1p-1h transitions. In this scenario we expand the eigenvectors $w_{\boldsymbol{\mu},\gamma}$ of Eq. (12a) in the direct products of the EKT-1 [Eq. (16)] eigenvectors $y_{i\sigma,\alpha}$ and $x_{j\sigma,\beta}$:

$$w_{\boldsymbol{\mu},\gamma} \equiv w_{ij\sigma,\gamma} = \sum_{\alpha\beta} C^{\sigma}_{\alpha\beta,\gamma}\, y_{i\sigma,\alpha} x_{j\sigma,\beta}. \tag{31}$$

We now exploit the fact that $y_{i\sigma,\alpha}$ and $x_{j\sigma,\beta}$ are also approximate eigenvectors of Eqs. (16). This allows us to recast Eq. (12a) in the form involving maximum the 2-RDMs:

$$\begin{aligned}&\sum_{\alpha\beta}\left\{[\epsilon^{(-)}_\beta + \epsilon^{(+)}_\alpha] \sum_{ij,\sigma} \big\langle \widehat{E}^{\sigma'}_{kl}\, \widehat{E}^{\sigma}_{ij}\big\rangle y_{i\sigma,\alpha} x_{j\sigma,\beta} + \mathcal{H}^{\sigma'\sigma}_{kl,\alpha\beta}\right\} C^{\sigma}_{\alpha\beta,\gamma} \\ &\quad = \epsilon^{(0)}_\gamma \sum_{\alpha\beta}\left\{\sum_{ij\sigma} \big\langle \widehat{E}^{\sigma'}_{kl}\, \widehat{E}^{\sigma}_{ij}\big\rangle y_{i\sigma,\alpha} x_{j\sigma,\beta}\right\} C^{\sigma}_{\alpha\beta,\gamma}, \qquad (32)\end{aligned}$$

where the matrix elements of the effective Hamiltonian are given in accordance with Eq. (29) by

$$\mathcal{H}^{\sigma'\sigma}_{kl,\alpha\beta} = \langle \widehat{E}^{\sigma'}_{kl} \mathcal{H}^{+}_{\alpha\beta} \rangle = \left(t^{\sigma}_{\beta\alpha} - \epsilon^{-}_{\alpha}\delta^{\sigma}_{\beta\alpha}\right)\langle \widehat{E}^{\sigma'}_{kl}\rangle + \sum_{cd}(\beta\alpha|cd)\langle \widehat{E}^{\sigma'}_{kl}\widehat{E}_{cd}\rangle - \sum_{cd}(c\alpha|\beta d)\langle \widehat{E}^{\sigma'}_{kl}\widehat{E}^{\sigma}_{cd}\rangle. \tag{33}$$

Here $t^{\sigma}_{\beta\alpha} = \sum_{ij} t_{ji} y_{i\sigma,\alpha} x_{j\sigma,\beta}$, and $\delta^{\sigma}_{\beta\alpha} = \sum_{ij}\delta_{ji} y_{i\sigma,\alpha} x_{j\sigma,\beta}$. If $\mathcal{H}$ is neglected, the excited-state energy is approximately equal to the quasiparticle energy difference between the virtual and the occupied states:

$$\epsilon^{(0)}_{\gamma} \approx \epsilon^{(-)}_{\beta} + \epsilon^{(+)}_{\alpha} \equiv E^{(N-1)}_{\beta} + E^{(N+1)}_{\alpha} - 2E_0. \tag{34}$$

Notice that $\epsilon^{(\pm)}$ are the correlated energies that include the self-energy corrections, which are missing in the EOM approach [23]. While it is an important finding, one may argue that the approximation (34) trivially follows from the Bethe-Salpeter in which the ingredient single-particle Green's functions are fully renormalized, but the kernel is missing. The main achievement of Eq. (32) is, however, that the correction can be written in extremely simple form of a Hartree-Fock Hamiltonian averaged over the correlated density matrix; maximally the 2-RDM is required. For a single-determinant reference state, Eq. (32) reduces to the random phase approximation.

b. Neutral excitations as a sum of two singly excited states. Since the procedure has already been explained in details above, it is sufficient to present results for the effective Hamiltonian. In fact, its structure is well known from the EOM method:

$$\mathcal{H}^{-}_{\alpha\beta} = \sum_{\mu\nu}\left\{[\widehat{E}_{\nu},[\widehat{H},\widehat{E}_{\mu}]] - \epsilon^{(0)}_{\alpha}[\widehat{E}_{\nu},\widehat{E}_{\mu}]\right\} w_{\mu,\alpha} w_{\nu,\beta}. \tag{35}$$

With this ingredient, the final eigenvalue equation reads

$$\sum_{\alpha\beta}\left\{\left[\epsilon^{(0)}_{\beta} + \epsilon^{(0)}_{\alpha}\right] S_{\eta\zeta,\alpha\beta} + \mathcal{H}_{\zeta\eta,\alpha\beta}\right\} C_{\alpha\beta,\gamma} = \epsilon^{(0)}_{\gamma}\sum_{\alpha\beta} S_{\eta\zeta,\alpha\beta} C_{\alpha\beta,\gamma}, \tag{36}$$

with

$$S_{\eta\zeta,\alpha\beta} = \sum_{\mu\nu}\langle \widehat{E}_{\zeta}\widehat{E}_{\eta}\,\widehat{E}_{\mu}\widehat{E}_{\nu}\rangle w_{\mu,\alpha} w_{\nu,\beta}, \tag{37}$$

$$\mathcal{H}_{\eta\zeta,\alpha\beta} = \langle \widehat{E}_{\zeta}\widehat{E}_{\eta}\,\mathcal{H}^{-}_{\alpha\beta}\rangle. \tag{38}$$

Equation (36) has the same complexity as the equation of motion

$$\langle[\widehat{E}_{\zeta}\widehat{E}_{\eta},\ \partial(\widehat{E}_{\mu}\widehat{E}_{\nu})]\rangle w_{\mu\nu,\alpha} = \epsilon^{(0)}_{\alpha}\langle[\widehat{E}_{\zeta}\widehat{E}_{\eta},\ \widehat{E}_{\mu}\widehat{E}_{\nu}]\rangle w_{\mu\nu,\alpha}. \tag{39}$$

Although they both depend on the 4-RDM, it is expected that their accuracy will be different depending on the nature of the reference ground state. Detailed comparison of these two approaches will be a topic of further investigations.

V. CONCLUSIONS

The extended Koopmans theorem [30] and the equation of motion approach [29] are well-known tools to compute excited electronic states of many-body systems in terms of the ground-state reduced density matrices. Traditionally, EKT has been used to describe the quasiparticle states, whereas EOM is typically reduced to the random phase approximation and used in the Casida equation form for neutral excitations. Recently, the EOM approach has been used to perturbatively include double excitations in the TDDFT excited states calculations [37,38]. It is known, however, that EOM additionally relies on the consistency condition (2) and, therefore, lacks important self-energy corrections [23]. It is explicitly demonstrated here that EKT includes these terms, which makes EKT an attractive tool to describe doubly excited configurations.

Motivated by these developments, we performed numerical simulations and demonstrated that the EKT theory is significantly more accurate than EOM or related configuration interaction methods of equivalent complexity, and even at the lowest level is capable of treating double electron excitations. Furthermore, connections between EKT and EOM have been analytically established on various levels: for a single-determinant ground state (Sec. II B) and for composite excitations (Sec. IV). This latter result leads to a method for the determination of excited states distinct from EOM, but of comparable complexity.

Since our theory requires only the ground-state quantities, it is especially relevant for extended systems where excited-state calculations using wave-function formalism are hard [65], but RDMs may be available from the Green's function methods [27,66]. Applications to systems involved in fast photophysical processes, such as polyenes where conical intersections are prevalent, are envisioned [67].

ACKNOWLEDGMENTS

Support of the German Research Foundation (Deutsche Forschungsgemeinschaft, DFG), Collaborative Research Centre SFB/TRR 173 "Spin+X" is acknowledged.

APPENDIX: TABULATED DATA

In Table I a compilation of numerical data for the lowest singlet state is shown.

TABLE I. Energies (in atomic units) and spectral strengths (dimensionless) of the first singlet excited state from the full CI, EKT-4, EKT-2, and CISD methods. $T_{\mathrm{SVD}} = 10^{-3}$ cutoff is used for all EKT calculations. Mean absolute errors of the excitation energy and spectral weight computed according to Eq. (24) are shown in the last row. These values can be directly compared with Fig. 3.

	Full CI		EKT-4		EKT-2		CISD	
$R_{\mathrm{O\text{-}H}}$	E	Z	E	Z	E	Z	E	Z
0.55	0.361579	0.973287	0.361627	0.973385	0.378146	0.990086	0.362804	0.970925
0.60	0.359150	0.974111	0.359192	0.974215	0.375409	0.990651	0.360443	0.971678
0.65	0.356718	0.974780	0.356769	0.974916	0.372834	0.991224	0.358069	0.972314
0.70	0.354188	0.975260	0.354257	0.975448	0.370347	0.991801	0.355595	0.972784
0.75	0.351483	0.975505	0.351580	0.975770	0.367916	0.992393	0.352955	0.973031
0.80	0.348530	0.975457	0.348662	0.975820	0.365556	0.993043	0.350086	0.972983
0.85	0.345228	0.975012	0.345320	0.975251	0.363366	0.993865	0.346908	0.972520
0.90	0.341261	0.973913	0.341327	0.974084	0.357394	0.991758	0.343135	0.971340
0.95	0.334962	0.971198	0.335005	0.971302	0.351588	0.990170	0.337088	0.968311
1.00	0.322777	0.964905	0.322840	0.965074	0.339534	0.984871	0.324940	0.961315
1.05	0.306016	0.955391	0.306095	0.955616	0.322284	0.975619	0.308001	0.951210
1.10	0.287490	0.943909	0.287578	0.944164	0.302794	0.963683	0.289277	0.939429
1.15	0.268013	0.930665	0.268097	0.930911	0.281912	0.949419	0.269617	0.926089
1.20	0.248050	0.915649	0.248123	0.915868	0.260306	0.933102	0.249490	0.911102
1.25	0.228063	0.898909	0.228124	0.899095	0.238647	0.915016	0.229362	0.894466
1.30	0.208468	0.880573	0.208518	0.880725	0.217482	0.895418	0.209646	0.876275
1.35	0.189591	0.860840	0.189630	0.860963	0.197200	0.874555	0.190669	0.856710
1.40	0.171665	0.839966	0.171696	0.840064	0.178055	0.852681	0.172660	0.836013
1.45	0.154841	0.818245	0.154862	0.818320	0.160191	0.830069	0.155770	0.814470
1.50	0.139207	0.795995	0.139223	0.796055	0.143680	0.807009	0.140084	0.792396
1.55	0.124798	0.773541	0.124810	0.773589	0.128536	0.783801	0.125637	0.770114
1.60	0.111614	0.751203	0.111623	0.751241	0.114740	0.760744	0.112426	0.747943
1.65	0.099626	0.729278	0.099633	0.729308	0.102244	0.738124	0.100423	0.726180
1.70	0.088787	0.708033	0.088792	0.708056	0.090983	0.716202	0.089580	0.705093
1.75	0.079036	0.687694	0.079041	0.687710	0.080882	0.695203	0.079834	0.684909
1.80	0.070303	0.668442	0.070307	0.668455	0.071860	0.675309	0.071115	0.665809
1.85	0.062515	0.650410	0.062519	0.650420	0.063832	0.656657	0.063348	0.647927
1.90	0.055595	0.633685	0.055600	0.633692	0.056714	0.639339	0.056458	0.631351
1.95	0.049467	0.618311	0.049471	0.618315	0.050422	0.623404	0.050366	0.616123
2.00	0.044057	0.604296	0.044061	0.604296	0.044877	0.608862	0.045000	0.602251
2.05	0.039294	0.591613	0.039299	0.591611	0.040002	0.595691	0.040288	0.589710
2.10	0.035112	0.580212	0.035117	0.580216	0.035728	0.583841	0.036163	0.578446
2.15	0.031448	0.570025	0.031453	0.570025	0.031987	0.573243	0.032562	0.568392
2.20	0.028244	0.560968	0.028250	0.560972	0.028720	0.563815	0.029428	0.559464
2.25	0.025448	0.552953	0.025453	0.552954	0.025872	0.555476	0.026709	0.551573
2.30	0.023009	0.545886	0.023016	0.545888	0.023390	0.548108	0.024357	0.544625
2.35	0.020886	0.539676	0.020892	0.539677	0.021230	0.541631	0.022327	0.538528
2.40	0.019038	0.534235	0.019044	0.534232	0.019352	0.535953	0.020581	0.533194
2.45	0.017428	0.529478	0.017435	0.529472	0.017718	0.530988	0.019083	0.528539
2.50	0.016026	0.525328	0.016032	0.525320	0.016296	0.526655	0.017803	0.524487
MAE	0.000000	0.000000	0.000034	0.000092	0.007275	0.010766	0.001277	0.002721

[1] G. Onida, L. Reining, and A. Rubio, Electronic excitations: density-functional versus many-body Green's-function approaches, Rev. Mod. Phys. **74**, 601 (2002).

[2] G. D. Scholes and G. Rumbles, Excitons in nanoscale systems, Nature Mater. **5**, 683 (2006).

[3] E. Runge and E. K. U. Gross, Density-Functional Theory for Time-Dependent Systems, Phys. Rev. Lett. **52**, 997 (1984).

[4] R. van Leeuwen, Causality and Symmetry in Time-Dependent Density-Functional Theory, Phys. Rev. Lett. **80**, 1280 (1998).

[5] *Time-Dependent Density Functional Theory*, Lecture Notes in Physics No. 706, edited by M. A. L. Marques (Springer, Berlin, 2006).

[6] G. Stefanucci and S. Kurth, Towards a Description of the Kondo Effect Using Time-Dependent Density-Functional Theory, Phys. Rev. Lett. **107**, 216401 (2011).

[7] S. Botti, A. Schindlmayr, R. D. Sole, and L. Reining, Time-dependent density-functional theory for extended systems, Rep. Prog. Phys. **70**, 357 (2007).

[8] C. Adamo and D. Jacquemin, The calculations of excited-state properties with Time-Dependent Density Functional Theory, Chem. Soc. Rev. **42**, 845 (2013).

[9] A. D. Laurent, C. Adamo, and D. Jacquemin, Dye chemistry with time-dependent density functional theory, Phys. Chem. Chem. Phys. **16**, 14334 (2014).

[10] D. Jacquemin, I. Duchemin, and X. Blase, Is the Bethe-Salpeter formalism accurate for excitation energies? Comparisons with TD-DFT, CASPT2, and EOM-CCSD, J. Phys. Chem. Lett. **8**, 1524 (2017).

[11] G. D. Scholes, G. R. Fleming, A. Olaya-Castro, and R. van Grondelle, Lessons from nature about solar light harvesting, Nature Chem. **3**, 763 (2011).

[12] R. Spezia, S. Knecht, and B. Mennucci, Excited state characterization of carbonyl containing carotenoids: a comparison between single and multireference descriptions, Phys. Chem. Chem. Phys. **19**, 17156 (2017).

[13] N. T. Maitra, Perspective: Fundamental aspects of time-dependent density functional theory, J. Chem. Phys. **144**, 220901 (2016).

[14] R. J. Cave, F. Zhang, N. T. Maitra, and K. Burke, A dressed TDDFT treatment of the 2^1A_g states of butadiene and hexatriene, Chem. Phys. Lett. **389**, 39 (2004).

[15] M. Huix-Rotllant, A. Ipatov, A. Rubio, and M. E. Casida, Assessment of dressed time-dependent density-functional theory for the low-lying valence states of 28 organic chromophores, Chem. Phys. **391**, 120 (2011).

[16] Y. Yang, D. Peng, J. Lu, and W. Yang, Excitation energies from particle-particle random phase approximation: Davidson algorithm and benchmark studies, J. Chem. Phys. **141**, 124104 (2014).

[17] O. V. Gritsenko, Expectations of the Kohn-Sham operator in a natural-orbital functional environment: An adiabatic response theory with single and double excitations, Phys. Rev. A **96**, 032507 (2017).

[18] Zeng-hui Yang, A. Pribram-Jones, K. Burke, and C. A. Ullrich, Direct Extraction of Excitation Energies from Ensemble Density-Functional Theory, Phys. Rev. Lett. **119**, 033003 (2017).

[19] C. A. Ullrich, U. J. Gossmann, and E. K. U. Gross, Time-Dependent Optimized Effective Potential, Phys. Rev. Lett. **74**, 872 (1995).

[20] R. van Leeuwen, The Sham-Schlüter Equation in Time-Dependent Density-Functional Theory, Phys. Rev. Lett. **76**, 3610 (1996).

[21] A. Marini and R. Del Sole, Dynamical Excitonic Effects in Metals and Semiconductors, Phys. Rev. Lett. **91**, 176402 (2003).

[22] G. Pal, Y. Pavlyukh, W. Hübner, and H. C. Schneider, Optical absorption spectra of finite systems from a conserving Bethe-Salpeter equation approach, Eur. Phys. J. B **79**, 327 (2011).

[23] D. Sangalli, P. Romaniello, G. Onida, and A. Marini, Double excitations in correlated systems: A many-body approach, J. Chem. Phys. **134**, 034115 (2011).

[24] A.-M. Uimonen, G. Stefanucci, Y. Pavlyukh, and R. van Leeuwen, Diagrammatic expansion for positive density-response spectra: Application to the electron gas, Phys. Rev. B **91**, 115104 (2015).

[25] S. Kümmel and L. Kronik, Orbital-dependent density functionals: Theory and applications, Rev. Mod. Phys. **80**, 3 (2008).

[26] A. Stan, P. Romaniello, S. Rigamonti, L. Reining, and J. A. Berger, Unphysical and physical solutions in many-body theories: from weak to strong correlation, New J. Phys. **17**, 093045 (2015).

[27] Y. Pavlyukh, Padé resummation of many-body perturbation theories, Sci. Rep. **7**, 504 (2017).

[28] O. Gunnarsson, G. Rohringer, T. Schäfer, G. Sangiovanni, and A. Toschi, Breakdown of Traditional Many-Body Theories for Correlated Electrons, Phys. Rev. Lett. **119**, 056402 (2017).

[29] D. J. Rowe, Equations-of-motion method and the extended shell model, Rev. Mod. Phys. **40**, 153 (1968).

[30] D. W. Smith and O. W. Day, Extension of Koopmans theorem. I. Derivation, J. Chem. Phys. **62**, 113 (1975).

[31] M. Rosina, Application of the two-body density matrix of the ground state for calculations of some excited states, Int. J. Quantum Chem. **13**, 737 (1978).

[32] D. A. Mazziotti, Extraction of electronic excited states from the ground-state two-particle reduced density matrix, Phys. Rev. A **68**, 052501 (2003).

[33] L. Greenman and D. A. Mazziotti, Electronic excited-state energies from a linear response theory based on the ground-state two-electron reduced density matrix, J. Chem. Phys. **128**, 114109 (2008).

[34] H. van Aggelen, B. Verstichel, G. Acke, M. Degroote, P. Bultinck, P. W. Ayers, and D. Van Neck, Extended random phase approximation method for atomic excitation energies from correlated and variationally optimized second-order density matrices, Comput. Theor. Chem. **1003**, 50 (2013).

[35] K. Chatterjee and K. Pernal, Excitation energies from extended random phase approximation employed with approximate one- and two-electron reduced density matrices, J. Chem. Phys. **137**, 204109 (2012).

[36] J. Wambach, Damping of small-amplitude nuclear collective motion, Rep. Prog. Phys. **51**, 989 (1988).

[37] N. T. Maitra, F. Zhang, R. J. Cave, and K. Burke, Double excitations within time-dependent density functional theory linear response, J. Chem. Phys. **120**, 5932 (2004).

[38] M. E. Casida, Propagator corrections to adiabatic time-dependent density-functional theory linear response theory, J. Chem. Phys. **122**, 054111 (2005).

[39] K. Pernal, K. Chatterjee, and P. H. Kowalski, How accurate is the strongly orthogonal geminal theory in predicting excitation energies? Comparison of the extended random phase approximation and the linear response theory approaches, J. Chem. Phys. **140**, 014101 (2014).

[40] R. C. Morrison, Extended Koopmans theorem ionization potentials for beryllium atom shake-up transitions, Int. J. Quantum Chem. **49**, 649 (1994).

[41] J. Cioslowski, P. Piskorz, and G. Liu, Ionization potentials and electron affinities from the extended Koopmans theorem applied to energy-derivative density matrices: the EKTMPn and EKTQCISD methods, J. Chem. Phys. **107**, 6804 (1997).

[42] D. Vanfleteren, D. Van Neck, P. W. Ayers, R. C. Morrison, and P. Bultinck, Exact ionization potentials from wavefunction asymptotics: The extended Koopmans theorem, revisited, J. Chem. Phys. **130**, 194104 (2009).

[43] N. E. Dahlen and R. van Leeuwen, Self-consistent solution of the Dyson equation for atoms and molecules within a conserving approximation, J. Chem. Phys. **122**, 164102 (2005).

[44] A. Stan, N. E. Dahlen, and R. van Leeuwen, Fully self-consistent *GW* calculations for atoms and molecules, Europhys. Lett. **76**, 298 (2006).

[45] S. Verdonck, D. Van Neck, P. W. Ayers, and M. Waroquier, Characterization of the electron propagator with a *GW*-like self-energy in closed-shell atoms, Phys. Rev. A **74**, 062503 (2006).

[46] M. Schüler and Y. Pavlyukh, Spectral properties from Matsubara Green's function approach: Application to molecules, Phys. Rev. B **97**, 115164 (2018).

[47] M. E. Casida, Time-dependent density functional response theory for molecules, in *Recent Advances In Density Functional Methods: (Part I)* (World Scientific, Singapore, 1995), pp. 155–192.

[48] R. van Meer, O. V. Gritsenko, and E. J. Baerends, Natural excitation orbitals from linear response theories: Time-dependent density functional theory, time-dependent Hartree-Fock, and time-dependent natural orbital functional theory, J. Chem. Phys. **146**, 044119 (2017).

[49] P. W. Ayers and J. Melin, Computing the Fukui function from *ab initio* quantum chemistry: approaches based on the extended Koopmans theorem, Theor. Chem. Acc. **117**, 371 (2007).

[50] A. Szabo, *Modern Quantum Chemistry: Introduction to Advanced Electronic Structure Theory* (Dover Publications, Mineola, 1996).

[51] D. A. Mazziotti, *Reduced-Density-Matrix Mechanics: With Application to Many-Electron Atoms and Molecules*, Advances in Chemical Physics, Vol. 134 (John Wiley & Sons, Hoboken, 2007).

[52] J. D. Farnum and D. A. Mazziotti, Extraction of ionization energies from the ground-state two-particle reduced density matrix, Chem. Phys. Lett. **400**, 90 (2004).

[53] D. A. Mazziotti, Approximate solution for electron correlation through the use of Schwinger probes, Chem. Phys. Lett. **289**, 419 (1998).

[54] Y. Pavlyukh and W. Hübner, Configuration interaction approach for the computation of the electronic self-energy, Phys. Rev. B **75**, 205129 (2007).

[55] J. W. Snyder and D. A. Mazziotti, Conical intersection of the ground and first excited states of water: Energies and reduced density matrices from the anti-hermitian contracted Schrödinger equation, J. Phys. Chem. A **115**, 14120 (2011).

[56] Y. Pavlyukh and J. Berakdar, Accessing electronic correlations by half-cycle pulses and time-resolved spectroscopy, Phys. Rev. A **90**, 053417 (2014).

[57] B. G. Levine, C. Ko, J. Quenneville, and T. J. Martínez, Conical intersections and double excitations in time-dependent density functional theory, Mol. Phys. **104**, 1039 (2006).

[58] P. Romaniello, D. Sangalli, J. A. Berger, F. Sottile, L. G. Molinari, L. Reining, and G. Onida, Double excitations in finite systems, J. Chem. Phys. **130**, 044108 (2009).

[59] Y. Pavlyukh and J. Berakdar, Electron repulsion integrals for self-energy calculations, Comput. Phys. Commun. **184**, 387 (2013).

[60] P. J. Knowles and N. C. Handy, A new determinant-based full configuration interaction method, Chem. Phys. Lett. **111**, 315 (1984).

[61] J. Olsen, B. O. Roos, P. Jørgensen, and H. J. Aa Jensen, Determinant based configuration interaction algorithms for complete and restricted configuration interaction spaces, J. Chem. Phys. **89**, 2185 (1988).

[62] M. E. Casida and M. Huix-Rotllant, Progress in time-dependent density-functional theory, Annu. Rev. Phys. Chem. **63**, 287 (2012).

[63] T. Deilmann, M. Drüppel, and M. Rohlfing, Three-particle correlation from a Many-Body Perspective: Trions in a Carbon Nanotube, Phys. Rev. Lett. **116**, 196804 (2016).

[64] Y. Pavlyukh, M. Schüler, and J. Berakdar, Single- or double-electron emission within the Keldysh nonequilibrium Green's function and Feshbach projection operator techniques, Phys. Rev. B **91**, 155116 (2015).

[65] J. McClain, J. Lischner, T. Watson, D. A. Matthews, E. Ronca, S. G. Louie, T. C. Berkelbach, and G. K.-L. Chan, Spectral functions of the uniform electron gas via coupled-cluster theory and comparison to the *GW* and related approximations, Phys. Rev. B **93**, 235139 (2016).

[66] Y. Pavlyukh, A.-M. Uimonen, G. Stefanucci, and R. van Leeuwen, Vertex Corrections for Positive-Definite Spectral Functions of Simple Metals, Phys. Rev. Lett. **117**, 206402 (2016).

[67] A. J. Musser, M. Liebel, C. Schnedermann, T. Wende, T. B. Kehoe, A. Rao, and P. Kukura, Evidence for conical intersection dynamics mediating ultrafast singlet exciton fission, Nat. Phys. **11**, 352 (2015).